Surface-Enhanced Nitrate Photolysis on Ice.

Guillaume Marcotte[1], Patrick Marchand[1], Stéphanie Pronovost[1], Patrick Ayotte[1,*], Carine Laffon[2] and Philippe Parent[2,*]

[1]Département de chimie, Université de Sherbrooke, 2500, boul. de l'Université, Sherbrooke (Québec) Canada J1K 2R1.

[2] CINaM-CNRS Campus de Luminy Case 913 13288 Marseille, France.

Abstract: Heterogeneous nitrates photolysis is the trigger for many chemical processes occurring in the polar boundary layer and is widely believed to occur in a quasi-liquid layer (QLL) at the surface of ice. The dipole forbidden character of the electronic transition relevant to boundary layer atmospheric chemistry and the small photolysis/photoproducts quantum yields in ice (and in water) may confer a significant enhancement and interfacial specificity to this important photochemical reaction at the surface of ice. Using amorphous solid water films at cryogenic temperatures as models for the disordered interstitial air/ice interface within the snowpack suppresses the diffusive uptake kinetics thereby prolonging the residence time of nitrate anions at the surface of ice. This approach allows their slow heterogeneous photolysis kinetics to be studied providing the first direct evidence that nitrates adsorbed onto the first molecular layer at the surface of ice are photolyzed more effectively than those dissolved within the bulk. Vibrational spectroscopy allows the ~3-fold enhancement in photolysis rates to be correlated with the nitrates' distorted intramolecular geometry thereby hinting at the role played by the greater chemical heterogeneity in their solvation environment at the surface of ice than in the bulk. A simple 1D kinetic model suggests 1-that a 3(6)-fold enhancement in photolysis rate for nitrates adsorbed onto the ice surface could increase the photochemical NO_2 emissions from a 5(8) nm thick photochemically active interfacial layer by 30%(60)%, and 2-that 25%(40%) of the NO_2 photochemical emissions to the snowpack interstitial air are released from the top-most molecularly thin surface layer on ice. These findings may provide a new paradigm for heterogeneous (photo)chemistry at temperatures below those required for a QLL to form at the ice surface.

Keywords: Ice surface (photo)chemistry; heterogeneous nitrate photolysis; photochemical NO_x fluxes; snowpack and polar boundary layer chemistry.

*Corresponding authors:
Patrick.Ayotte@USherbrooke.ca; Tel.: 1-819-821-7889;
parent@cinam.univ-mrs.fr; Tel.: 33 (0)6 60 30 28 07.

I. Introduction: About 15 years ago, the snowpack was identified as an unexpectedly intense source of NO_x ($NO+NO_2$)[1] resulting in their surprisingly high mixing ratios[2] at the high latitude polar boundary layer over heretofore considered unpolluted regions (e.g., Summit, Greenland). The demonstration that homogeneous gas phase chemistry[2] was unable to account for this phenomenon hinted towards a heterogeneous (photo)chemical source within the sunlit snowpack thereby triggering widespread scientific interest. Many subsequent field campaigns [e.g., ISCAT,[3] ANTCI,[4] CHABLIS[5]] later demonstrated that intense photochemical NO_x fluxes emanating from snow are ubiquitous. In agreement with expectations from aqueous nitrates photochemistry, the primary event responsible for the phenomenon was soon attributed to the photolysis of snow-bound nitrates.[6,7] However, the distribution of nitrates in natural snow is complex, extremely heterogeneous and involves a very diverse speciation (sea salt, mineral dust, etc.). This may therefore be responsible for the highly variable amounts of photo-labile and photo-stable nitrates fractions which provide contributions to the photochemical NO_x fluxes arising from the surface or the bulk of ice and snow, from liquid and solid domains, from micro-inclusions or grain boundaries, thereby complicating comparisons between observations from different locations. Therefore, laboratory investigations have been devised using natural samples[8,9] or nitrates-doped artificial snow/ice samples[10–15] to study the phenomenon at the molecular/mesoscopic levels under more controlled conditions. This is necessary in order to quantify the relevant physico-chemical parameters that could more appropriately describe the photolysis of snow-bound nitrates.[16,17] Given all these difficulties, it is not surprising that the magnitude of the photochemical NO_x fluxes predicted by atmospheric chemistry models of the polar boundary layer remains contentious illustrating the fact that our understanding of heterogeneous (photo)chemistry in snow is incomplete.

For example, the prevailing view has it that snow (photo)chemistry occurs almost exclusively in a quasi-liquid layer (QLL), that resides at the air-ice interface within the porous snowpack, and where snow-bound impurities are completely segregated, either because of their limited solubility in crystalline ice, because they adsorbed from the gas phase, or because of their intrinsic surface activity (i.e., excess surface Gibbs energy).[17–20] Accordingly, the concentration of impurities in the QLL and its thickness (at the polar boundary layer temperature) are usually derived from the snow *bulk* composition using thermodynamic models. Finally, snow (photo)chemistry in the QLL is largely understood in terms of aqueous phase mechanisms and rates.[18,19,21] While model results are often reported to reproduce field observations of NO_x fluxes and/or mixing ratio, agreement is sometimes deceiving as model parameters, such as ice/QLL partitioning or (photo)chemical kinetic parameters, are often so poorly constrained that they are treated as adjustable parameters in some models.[22] Furthermore, while recent reports have shown that only at temperatures very near the melting point of ice ($T>-1{,}5^oC$) is a QLL present at the air/single crystalline ice interface,[23,24] it is clear that strong photochemical NO_x fluxes are observed to emanate from the snowpack even at temperatures (i.e., 240 K-260 K) where the extent (i.e., coverage and thickness) of the QLL is expected to be very limited.[25] Finally, while the conditions required to favor the occurrence of a QLL on ice are still being

debated, it has been recently advocated, based on simple physical considerations, that the extent of the QLL coverage at the air-ice interface on snow at the temperature of the polar boundary layer was much overestimated by these approximations.[26] At these much colder temperatures (i.e., T<263 K), a molecularly-thin disordered/defective interfacial layer must nonetheless exist at the interstitial air/ice interface whose properties must be better understood as it mediates pollutants adsorption and the heterogeneous reactivity of snow.

In section II, we describe how amorphous solid water (ASW), the glassy extension of deeply supercooled liquid water,[27,28] is used as a model for the disordered interstitial air/ice interface within the snowpack. Cryogenic temperatures suppress diffusive uptake kinetics, allowing the residence time of nitrate anions at the surface to be extended. This enables their slow photolysis kinetics to be studied and compared with those of nitrates dissolved within the bulk. We demonstrate, in section III.A, that nitrate anions adsorbed onto the first molecular layer on ice are photolyzed up to nearly three times more effectively than those dissolved within the bulk. While vibrational spectroscopy allows some of this enhancement in photolysis rates to be linked to the distorted intramolecular geometry of NO_3^- (which relaxes the dipole forbidden character of the $n \rightarrow \pi^*$ transition indicating that the surface of ASW presents a much more heterogeneous solvation environment than the bulk), contributions from enhanced photolysis quantum yields at the interface cannot be ruled out. Furthermore, we also demonstrate, using a simple kinetic model described in Section III.B, that a 3(6)-fold enhancement in nitrate anions photolysis rate at the surface of ice increases the photochemical NO_2 emissions from a very thin (<10 nm) photochemically active layer at the surface of ice to the snowpack interstitial air by 30%(60%). Model results also suggest that 25%(40%) of the NO_2 emissions from ice to the snowpack interstitial air could emanate from the top-most molecularly thin surface layer on ice. While atmospheric chemists have long suspected there exists a propensity for (photo)chemical processes to be enhanced at aqueous surfaces, the methodology described herein enables the first direct observation that nitrate anions are photolyzed more effectively at aqueous interfaces than in the bulk. Furthermore, our proposal of the formation of a thin photochemically active surface layer on ice, resulting from the complex coupled interfacial kinetics (i.e., NO_2 adsorption, desorption, diffusive uptake and hydrolysis as well as NO_3^- photolysis and diffusion), could provide a new perspective for describing heterogeneous (photo)chemistry on ice and its role in polar boundary layer chemistry at temperatures below those required for a QLL to form at the ice surface.

II. Experimental: Experimental studies of the slow heterogeneous nitrates (photo)chemistry on snow remain extremely challenging due to the high H_2O vapor pressure of ice and the (comparatively) rapid bulk uptake of nitrates by ice. Using model systems, laboratory studies have previously reported NO_3^- photolysis to be independent of ice film thickness[12] while field work showed NO_x fluxes increase with the specific surface area of the snow.[29] Both these observations hint at a significant contribution from the photolysis of surface-bound nitrates to the total photochemical NO_x fluxes from snow. While previous studies have reported NO_3^- photolysis was enhanced at the surface of thin films of water or ice,[30–34] these reports either relied on indirect evidence, or could not

differentiate surface photolysis from bulk photolysis, nor their relative contributions to the observed effective photolysis rates or photoproducts yields. Given these compelling yet somewhat indirect evidences, we are poised to provide direct evidence for enhanced NO_3^- photolysis at the surface of ice. However, highlighting any interfacial specificity in molecular-level reaction mechanisms[15,31,32,34–37] or in their kinetics[37–40] requires means of discriminating processes occurring on the surface from those occurring in the bulk. As nitrates photolysis kinetics are very slow,[10,41,42] any specific contribution from surface-bound NO_3^- may be obscured by diffusive uptake into the bulk which, however slow,[51] will strongly couple the surface and bulk contributions to the overall photolysis rates and photochemical NO_2 fluxes. In most laboratory or natural ice/snow samples, this yields an average photolysis rate which, at best, only yields a slight enhancement due to their modest specific surface area. To highlight any contribution arising specifically from the surface, the slow photolysis and diffusive uptake kinetics of nitrates in/on ice must therefore be decoupled.

In this work, all these shortcomings are overcome: 1 - by using amorphous solid water films (ASW) at cryogenic temperatures (i.e., T<120 K) as model systems to contrast and compare the photolysis rates of NO_3^- adsorbed onto the first molecular layer at a disordered ice surface with that of NO_3^- dissolved within the bulk, and 2 - by using vibrational spectroscopy to directly monitor, *in situ* and in real time, the photo-destruction of NO_3^- in either "surface" nitrates samples or "bulk" nitrates samples during UV irradiation with a Xe lamp. In addition, vibrational spectroscopy also enabled the intramolecular NO_3^- geometrical distortions and symmetry to be probed,[43] through its effects on the asymmetric NO stretching vibrations (hereafter, asym-$NO_{str.}$) of surface nitrates or bulk nitrates, providing important information on their local solvation environment. Indeed, the isolated gas phase anion[44] yields a single spectral feature for the asym-NO_{str} vibrations in cold $NO_3^-\cdot Ar_n$ (i.e., degenerate in the D_{3h} point group) that splits into two distinct bands upon hydration in $NO_3^-\cdot(H_2O)_n$.[45] Symmetry breaking is also well-known to occur when nitrates form ion-pairs with a hard cation (e.g., Ca^{2+}) in aqueous solutions resulting in an increased asym-$NO_{str.}$ splitting.[46] The asym-NO_{str} vibrations are therefore a convenient proxi for symmetry breaking in the nitrate anion[46–49] revealing chemical heterogeneity in its local solvation environments.[50] For this study, sample preparation and photolysis were performed at cryogenic temperatures (i.e., 70 K to 120 K) thereby allowing the diffusive transport kinetics, that may otherwise result in bulk uptake or surface segregation, phase separation, or even crystallization of the mixed binary amorphous solids, to be kinetically hindered.[51,52] Furthermore, adsorption of water vapor would rapidly blur contributions from nitrates adsorbed onto a dynamic air/ice interface. Studying the slow heterogeneous NO_3^- photolysis kinetics therefore also requires the adsorption and desorption of water vapour from the ice surface to be suppressed. Working under ultrahigh vacuum (UHV) conditions and at cryogenic temperatures provides the required conditions, thereby significantly extending the residence time of nitrates adsorbed onto the top-most layer at the surface of ice.

Amorphous binary HNO_3:H_2O samples were prepared using vapour condensation onto a polycrystalline gold substrate that could be cooled to a base temperature as low as

20 K by a closed-cycle helium cryostat. The temperature of the polycrystalline gold substrate was measured using a silicon diode and was controlled to within ±0,5 K (using the built-in PID algorithm on a model 332 Lakeshore temperature control unit). HNO_3 and H_2O vapours were supplied to a UHV ($P<10^{-9}$ torr) preparation chamber through separate leak valves and independent gas lines in order to minimize any mixing/reaction of the gases prior to their adsorption onto the substrate. Neat water vapour was supplied using the saturation vapour pressure over deionized H_2O which was degassed through at least three freeze-pump-thaw cycles. Anhydrous HNO_3 vapour was obtained from the vapour pressure over a H_2SO_4:HNO_3:H_2O ternary mixture (i.e., a 4:1 mixture of 96% sulfuric acid and 70% nitric acid solutions; Aldrich) which was also degassed by at least three freeze-pump-thaw cycles. The saturation vapour pressure over freshly prepared ternary mixtures was ~6 torr at 298 K and composed of >99% HNO_3 vapours (i.e., with <1% H_2O).[53] The preparation chamber was separated from the analysis chamber ($P<2x10^{-10}$ torr) by a gate valve allowing its complete evacuation after sample deposition and prior to its transfer to the analysis chamber.

"Surface nitrates" samples were prepared by sequential deposition of 10 L H_2O at 90 K (1 L ≡ 10^{-6} torr·s exposure), which was then heated to 120 K in order to relax any residual sample porosity.[54] The substrate was finally brought to the temperature of the UV photolysis experiment (i.e., either 70 K, 100 K or 120 K) prior to the exposure of the ice film to 0.4 L HNO_3. This surface coverage was chosen since it represents a reasonable compromise between improving the signal-to-noise ratio without, however, exceeding the saturation coverage for ionic dissociation of HNO_3 on amorphous ice.[52,55] "Bulk nitrates" samples were prepared by introducing HNO_3 and H_2O vapours simultaneously to the preparation chamber. The partial pressures of the two gases were adjusted to achieve the desired molar ratio (~5 % HNO_3 in H_2O; 100 L coverage films) in the condensed phase while the substrate temperature was set to 90 K during sample deposition in order to minimize sample porosity. The substrate was then finally brought to the temperature of the UV photolysis experiment (i.e., either 70 K, 100 K or 120 K).

All UV irradiations were performed with a 1000 W ozone-free Xe arc lamp (Oriel). The light flux from the lamp was transmitted to the sample through a 10 cm long water cooled filter (Oriel), sealed with quartz windows and filled with deionized water. This removed some of the infrared emissions from the Xe plasma thereby decreasing the thermal load on the sample. A UV grade fused silica plano-convex lens (70 cm focal length, Oriel) was used in order to further collimate the UV beam on the sample yielding about ~10 W of total output as measured by a thermopile detector. Irradiation of the HNO_3:H_2O binary amorphous films inside the analysis chamber was performed through a UV grade fused silica UHV port (Lesker). The substrate base temperature increased from 20 K to reach ~60 K under these irradiation conditions thereby limiting the lowest temperature at which nitrates photolysis could be studied reliably under thermally regulated conditions to $T \geq 70$ K.

The incident UV irradiance delivered to the sample within the UHV analysis chamber was evaluated by studying photolysis of 1.0 mM KNO_3 solutions in a thermally regulated 1 cm quartz SUPRASIL UV-grade cuvette.[56] In these experiments, the optical

setup was identical to that described above for irradiation within the analysis UHV chamber. Nitrates photolysis rates measured experimentally in aqueous solutions at 293 K agreed to within 33% with that calculated using the spectral irradiance of the ozone-free lamp provided by the manufacturer (scaled to the total lamp output power measured experimentally), along with the molar extinction coefficients of nitrates aqueous solutions at standard temperature and pressure, and nitrates photolysis quantum yields of 0.01.[57] More importantly however, photolysis rates were calculated with, and without, taking into account contributions from the strongly dipole-allowed $\pi \rightarrow \pi^*$ transition (i.e., $\lambda<270$nm). These simple calculations allowed us to estimate that photolysis in the $\pi \rightarrow \pi^*$ absorption band contributed no more than 20% to the photolysis rates reported herein (i.e., despite its molar absorptivity being more than three order of magnitude greater than those of the $n \rightarrow \pi^*$ absorption band).[57]

The UV beam (i.e., $\lambda>290$ nm) was shone at normal incidence on the substrate and was aligned to overlap with the focal spot of the FTIR spectrometer (Jasco) at the center of the UHV analysis chamber using a video camera. The evolution in chemical composition of samples submitted to UV irradiation was monitored *in situ* using reflection absorption infrared spectroscopy (RAIRS) performed at 85° incidence using the FTIR spectrometer. The reflectivity of the bare polycrystalline gold substrate was used as the background spectrum to calculate absorbance from the reflectivity of the mixed binary amorphous film/gold substrate system as a function of irradiation time. The (much more rapid) photolysis kinetics of neat solid HNO_3 were used as a relative calibration for day-to-day alignment of the UV beam with the IR beam of the FTIR spectrometer onto the gold substrate.

III. Results and discussion.

III.A Photolysis kinetics of "surface" nitrates and "bulk" nitrates.

Photolysis kinetics of nitrates in ice and in water are very slow, displaying photo-destruction half-lives of several hours under irradiation with high power UV lamps. The 1200-1575 cm^{-1} range of the RAIRS spectra for surface nitrates (A) and bulk nitrates (B) samples reported in Figure 1 reveal the subtle spectral evolutions in the asym-$NO_{str.}$ vibrational modes that result from UV photolysis for five hours at 70 K. Initially, the breadth of the asym-$NO_{str.}$ vibrational frequency distribution (black spectra) appears to be significantly greater for surface nitrates (A) than for bulk nitrates (B). After five hours of continuous UV irradiation (red spectra), both the bands' intensity and splitting have decreased, albeit much more significantly for surface nitrates (A) than for bulk nitrates (B). This is best illustrated by the arrows in Figure 1 that display the evolution in the bands' barycenter as a function of irradiation time. Unfortunately, attempts to identify the spectral signatures of the possible/expected nitrates photolysis reaction products with RAIRS[55] and NEXAFS[52] remain unsuccessful.

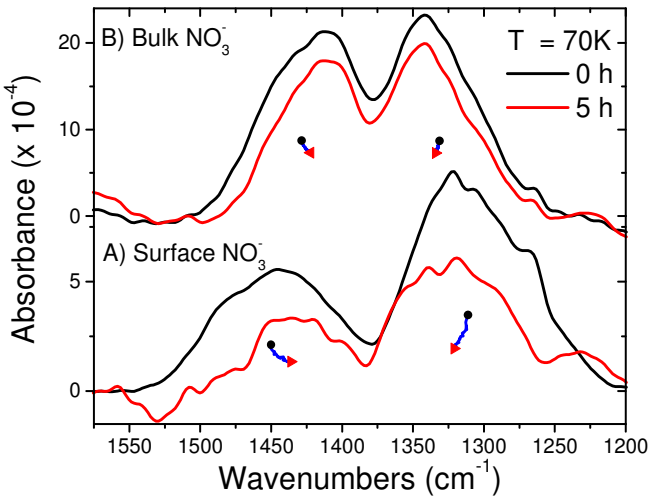

Fig. 1. Reflection-absorption infrared spectra of surface nitrates (A) and bulk nitrates (B) before (black) and after (red) 5 hours of UV irradiation at 70 K ($\lambda > 290$ nm, thereby mimicking solar radiation at sea level).[58] Surface nitrates samples were created by adsorbing 0,4 L HNO_3 onto a 10 L dense ASW film while bulk nitrates samples (~5% mole fraction) were prepared by simultaneous condensation of HNO_3 and H_2O vapours on a gold substrate under conditions known to yield extensive ionic dissociation of HNO_3.[39,41] Arrows indicate the path followed by the bands' barycenter, illustrating spectral evolution during irradiation.

The transition moments of the asym-NO_{str} vibrations vary but only very little as a function of intramolecular geometrical distortions.[49] The spectral features' integrated amplitudes were therefore used to infer the evolution of nitrates concentrations during UV irradiation. In Figure 2A, the relative abundances for surface nitrates (open symbols) and for bulk nitrates (filled symbols) are reported as a function of irradiation time at three temperatures: 70 K (black squares), 100 K (red circles), and 120 K (blue triangles). First-order photo-destruction kinetics were used to extract effective photolysis rate constants for surface nitrates (dashed lines) and bulk nitrates (continuous lines). These effective rate constants are reported in Figure 2B where it can be seen that, for the three temperatures investigated experimentally, the photolysis of surface nitrates (open bars) is significantly faster than that of bulk nitrates (filled bars) [i.e., an enhancement by a factor (2,7±0,6) is observed at 70 K]. Surprisingly, while the photolysis rates of bulk nitrates increase slightly with increasing temperature (filled bars), similarly to what is observed in ice and aqueous solutions,[10] those of surface nitrates decrease with increasing temperatures (open bars). At T=120 K, the surface nitrates photolysis rate is comparable to that of bulk nitrates.

The similarity between the NO_3^- photolysis rate for surface nitrates and bulk nitrates samples at 120 K could be due to the fact that, at this temperature, the onset of diffusive uptake kinetics has caused NO_3^- adsorbed onto the surface of the ASW film to be absorbed by the underlying substrate. Indeed, previous X-ray absorption[52] and infrared spectroscopic[55] studies have reported that NO_3^- anions (arising from ionic dissociation of HNO_3 adsorbed onto ASW) diffuse within the underlying substrate on an experimentally observable time scale at or near this temperature (i.e., albeit to a depth of <50 Å according

to Marcotte et al.).[52] Therefore, as nitrate anions cannot be kinetically trapped at the surface of ASW at 120 K, and because they have diffused within the ASW substrate, the behavior (i.e., photolysis rate, asym-NO_{str} splitting) of surface nitrates samples (Figure 2A, open blue triangles) is more akin to that of bulk nitrates samples (Figure 2A, filled blue triangles). Accordingly, the photo-destruction rates of NO_3^- anions in surface nitrates samples only displays a significant enhancement over those of bulk nitrates samples at 70 K and 100 K (Figure 2A and 2B). As transport kinetics are strongly suppressed at these temperatures, we conclude the increase in effective photo-destruction rates originates from the enhancement in heterogeneous photolysis of NO_3^- anions that remain adsorbed onto the top-most molecular layer at the surface of ice (i.e., as long as T<120 K).

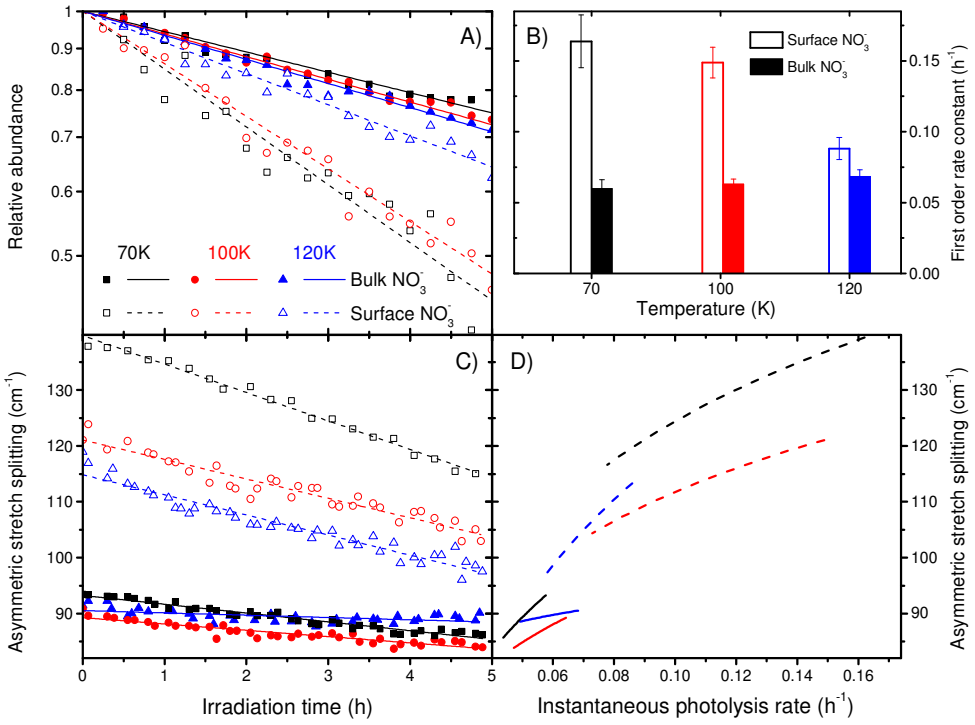

Fig. 2. Evolution of the relative abundance (panel A) and the asym-$NO_{str.}$ splitting (panel C) of surface nitrates (open symbols) and bulk nitrates (filled symbols) as a function of irradiation time during photolysis at 70 K (black squares), 100 K (red circles), and 120 K (blue triangles). Photolysis rates are obtained assuming first-order photo-destruction kinetics, for surface nitrates (dashed lines) and bulk nitrates (solid lines), and are reported in panel B (uncertainties at the 95% confidence level from least-square analysis). In panel C, linear trends in the asym-$NO_{str.}$ splitting (calculated from the bands' barycenters displayed in Figure 1) upon UV photolysis for surface nitrates (dashed lines) and bulk nitrates (solid lines) are reported. Panel D shows that a strong correlation exists between the instantaneous photodestruction rates (calculated from the decays in panel A) and the instantaneous asym-$NO_{str.}$ splitting (displayed in panel C).

Several factors could contribute to accelerate NO_3^- photolysis rates at the surface of ASW. For example, as adsorption onto condensed water interfaces only provides a partial solvation cage to nitrate anions, this could result in a more facile (i.e, compared to bulk photolysis) release of photoproducts to the gas phase (i.e., yielding greater photolysis/photoproducts quantum yields). Indeed, this was previously suggested to result in greater photolysis rates for nitrates adsorbed at wet surfaces than for those dissolved within the bulk.[33,36] Unfortunately, as for the present work,[59] the lack of surface nitrates absorption cross sections/extinction coefficients precluded an evaluation of their photolysis quantum yields.

Further insight into the molecular-level interpretation of this enhancement in photolysis rates for NO_3^- adsorbed onto ASW can be garnered upon closer scrutiny of the evolution in their vibrational fingerprint during UV irradiation of the samples. As observed in the vibrational spectra displayed in Figure 1, the splitting between the asym-$NO_{str.}$ vibrational features is significantly greater for surface nitrates samples than for bulk nitrates samples. To quantify this effect, the difference in the frequencies of the bands' barycenter for surface nitrates samples (open symbols) is compared with that for bulk nitrates sample (filled symbols) in figure 2C. The asym-$NO_{str.}$ splitting displayed by surface nitrates samples (i.e., 97-137 cm^{-1} in Figure 2C, open symbols) is much greater than that displayed by bulk nitrates samples (i.e., 84-94 cm^{-1} in Figure 2C, open symbols). This suggests that nitrate anions experience a greater chemical heterogeneity in their solvation environment at the surface of ice compared to the bulk.[43,50] Indeed, NO_3^- adsorption on aqueous interfaces was studied previously using electronic structure methods and their asym-$NO_{str.}$ splittings were shown to be strongly correlated with their intramolecular distortion[49,60] and to be of the same magnitude as those reported herein. Interestingly, splittings as large as 200-250 cm^{-1} are observed for the most distorted nitrates as can be gleaned from Figure 1. These splittings could be compared with those reported for concentrated $Ca(NO_3)_2$ solutions (i.e., 76 cm^{-1})[46] thereby suggesting that adsorption onto ice indeed results in a very strong intramolecular geometrical distortions, perhaps even exceeding those experienced in the first solvation sphere of a hard cation such as $Ca^{2+}_{(aq)}$. Finally, Figure 2C indicates that, while the asym-$NO_{str.}$ splitting displayed by bulk nitrates decreases only slightly over the 5 hours duration of the photolysis experiment [i.e., by less than 8 cm^{-1} at either 70 K (black squares), 100 K (red circles), or 120 K (blue triangles)], that displayed by surface nitrates decreases by at least twice as much (i.e., by more than 20 cm^{-1}) under the same conditions. This suggests there may exist a link between the increased NO_3^- intramolecular geometrical distortions and their enhanced photolysis rates.

This correlation is made more explicit in Figure 2D by plotting the instantaneous effective photo-destruction rates (from Figure 2A) as a function of the instantaneous asym-$NO_{str.}$ splitting (from Figure 2C) for bulk nitrates (continuous lines) and surface nitrates (dashed lines) at 70 K (black), 100 K (red) and 120 K (blue). As expected, the effective photolysis rates increase with increasing intramolecular geometrical distortions of the nitrate anions (for which the asym-$NO_{str.}$ splitting is used as a proxy). This suggests that the enhancement in heterogeneous NO_3^- photolysis on ice may be linked to a partial lifting in the strongly dipole-forbidden character of the $n \rightarrow \pi^*$ electronic transition induced by

symmetry breaking.[61,62] Indeed, complexation of nitrate anions to monovalent and divalent cations in aqueous solutions has been reported to cause intramolecular geometrical distortions, as evidenced by an increased asym-$NO_{str.}$ splitting,[46] and by shifts in their electronic spectrum.[46,63] Furthermore, increases in absorption cross sections for the $n \rightarrow \pi^*$ electronic transition (centered near 302 nm in aqueous solutions of nitrates) were reported in metal-nitrates solutions.[63] In addition, enhancements in UV absorption cross sections were also reported for HNO_3 upon adsorption on ice films (as well as on aluminium surfaces) compared to the gas phase but the physical origin of the enhancement (on ice) was not elucidated.[15] It is thus clear that increases in absorption cross sections, resulting from relaxed dipole selection rules arising from the increased intramolecular geometrical distortions at the air-ice interface, could enhance the photolysis rates for surface-bound nitrates compared to those dissolved within the bulk.

In summary, the surface of ASW provides a unique model system which allows the bulk and surface processes to be decoupled as transport kinetics are strongly inhibited at cryogenic temperatures. Furthermore, it also provides a kinetically frozen heterogeneous solvation environment which could resemble that transiently sampled by nitrate anions adsorbed onto the dynamically disordered ice-interstitial air interface within the porous snowpack at temperatures below those required for a QLL to form at the ice surface. The observations reported herein strongly suggest that chemical heterogeneities in the nitrate anions solvation environment at the ice surface result in significant intramolecular geometrical distortion. Given the strongly dipole forbidden character of the $n \rightarrow \pi^*$ electronic transition, the perturbed geometry of surface nitrate anions could result in an increased absorption cross section.[61,63] Furthermore, increased photolysis quantum yields for nitrate anions adsorbed onto ice could also contribute to the nearly three-fold enhancement in their photolysis rates compared to the bulk. In section III.B, we use kinetic modeling to investigate the contribution of such an (admittedly modest) enhancement in the photolysis rate of surface-bound nitrates (i.e., those NO_3^- anions adsorbed onto the top-most molecular layer at the surface of ice) to the photochemical NO_2 emissions to the snowpack interstitial air, which ultimately fuel the NO_2 fluxes that emanate from the sunlit snowpack to the polar boundary layer.

III.B Kinetic modeling of the photochemical NO_2 emissions from ice to the snowpack interstitial air.

While most models describe snow-bound impurities, and their (photo)chemistry, as essentially occurring exclusively in a superficial QLL,[18,19] this 1-D kinetic model (outlined in Figure 3, and described in details in the Supplementary Information) assumes that nitrates are distributed homogeneously in the bulk and surface layers of ice and that photolysis occurs throughout. It is important to stress that this simplified kinetic model is not intended to reproduce neither the (photo)chemical NO_x fluxes nor the interstitial air or polar boundary layer NO_2 mixing ratios observed in the field. Rather, its goal is to evaluate the relative magnitude of a possible contribution from enhanced photolysis of nitrates adsorbed onto the top-most surface layer on ice to the NO_2 mixing ratio in the snowpack interstitial air, on a typical windless summer day at the polar boundary layer, and at

temperatures where the QLL thickness and coverage are expected to be extremely limited (i.e., T~ 243 K). Accordingly, the model is parametrized (i.e., kinetic parameters used in the model are summarized in Table S1) to describe the coupled reaction and transport kinetics between bulk ice, and interstitial air though a molecularly thin interfacial ice layer (i.e., as opposed to a QLL) within which NO_3^- photolysis and NO_2 hydrolysis kinetics could be enhanced compared to the bulk. The physical dimensions used in the 1-D kinetic model are based on a mean ice crystal thickness of 10 μm and a snow porosity of 90%, in agreement with morphological parameters typical of fresh snow.[29] The concentration profiles and transport kinetics are discretized using 3000 layers having a thickness of 1.67 nm (i.e., corresponding to ~4.5 ice bilayers) and periodic boundary conditions are imposed. An initial NO_3^- concentration of 4.4 μM was selected[7,20,64] and, while the initial nitrates concentration is evenly distributed through the bulk and surface layers of the snow crystal, NO_3^- is obviously always totally absent from the gas phase. Interstitial air $NO_{2(g)}$ mixing ratio as well as surface and bulk concentrations were also initially set to zero. Diffusive transport kinetics between adjacent layers within bulk ice (Layers 2 to 3000) as well as with its surface layer (Layer 1) are described explicitly for NO_3^- and NO_2 using 1-D fickian diffusion. Finally, the kinetics for NO_2 adsorption onto, and desorption from, the surface layer of ice:

$$NO_{2(g)} \overset{K_{ads}}{\longleftrightarrow} NO_{2(ads)} \qquad \text{(R1)}$$

couple the condensed phase processes with those occurring in the gas phase. As they are much faster than all condensed phase processes involved, they are described using an equilibrium partition coefficient.[65]

The model is based on the simplified kinetic scheme illustrated in Figure 3 in which both NO_3^- photolysis[41]

$$NO_3^- \overset{h\nu}{\rightarrow} NO_2 + O^- \qquad \text{(R2)}$$

and NO_2 hydrolysis

$$NO_2 + NO_2 + H_2O \overset{\Delta}{\rightarrow} H^+ + NO_3^- + HONO \quad \text{(R3)}$$

occur throughout bulk ice (*bulk* rate constants are used for Layers 2 to 3000, see Table S1). In the model, nitrate anions are supplied to the ice surface (i.e., Layer 1) either as a result of heterogeneous NO_2 hydrolysis (R3), or through NO_3^- diffusion from the bulk to the surface layer, whereby they may transiently experience the chemically heterogeneous solvation environment (i.e., yielding intramolecular geometrical distortions and/or increased quantum yields) responsible for their enhanced photolysis. *Surface-specific* rate constants could thus be assigned to Layer 1 (which is NOT a QLL) allowing to account for *enhanced* heterogeneous NO_2 hydrolysis[38,39,66] and *enhanced* heterogeneous NO_3^- photolysis in the single, top-most surface layer on ice (See Table S1). While the model is intended to investigate the effects of a 3(6)-fold enhancement in heterogeneous nitrates photolysis rates (i.e., over the bulk nitrates photolysis rates of Galbavy et al.[41]), we caution that the enhancement in photolysis rates for NO_3^- anions that reside transiently at the

dynamic interstitial air/ice interface within the snowpack at 243 K might well be different. When temperature-dependent rates were available, a temperature of 243 K (i.e., -30°C) was assumed. The effect of diurnal cycles in the actinic flux is modeled by modulating the nitrates photolysis rates according to field observations.[58] Finally, the kinetic master equation describing these coupled elementary transport (diffusion, adsorption and desorption) and reactive (photolysis and hydrolysis) processes was numerically integrated over the diurnal cycles in the actinic flux using a 3.6 s time-step. Identical results were obtained using a 3.6 ms time-step in a few shorter simulations.

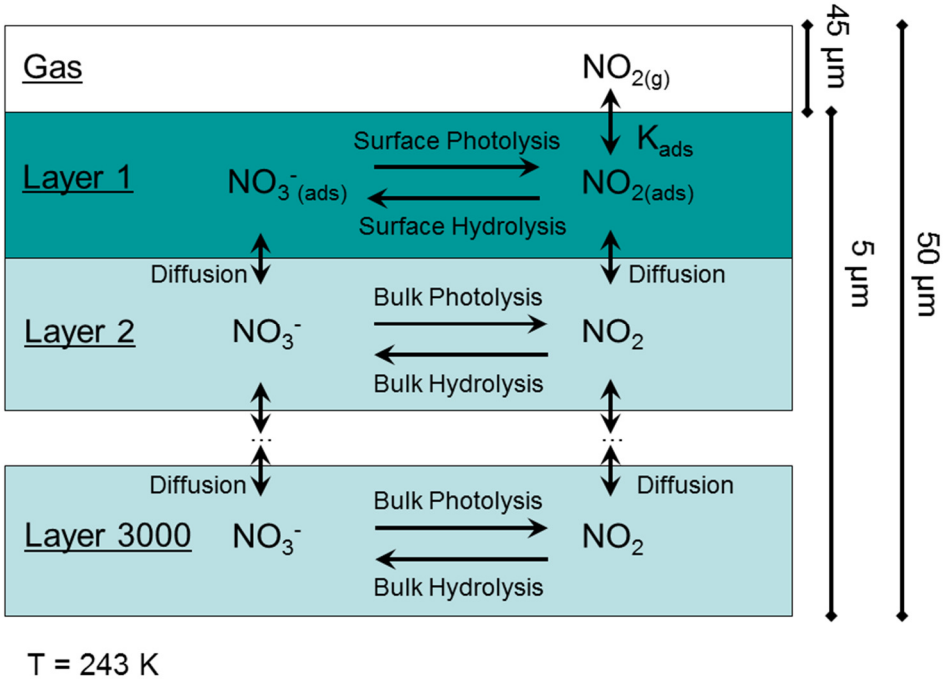

Fig. 3. Schematics of the simplified kinetic scheme used to describe the contribution of enhanced nitrate photolysis rates at the surface of ice to the photochemical NO_2 emissions to the snowpack interstitial air at 243 K.

Briefly, the model (Figure S1) indicates that, within a few hours, bulk nitrates photolysis ($t_{½}$~36.5 days for the noon-time actinic flux; Figure S2A) builds up the bulk NO_2 concentration in ice (Figure S2B) until a photochemical quasi-stationary state is established with bulk NO_2 hydrolysis [$t_{½}$~2.6 (6.9) h using the steady state noon-time (night-time) bulk NO_2 concentrations]. In the surface layer, the NO_2 hydrolysis rate constant is about six orders of magnitude larger (Table S1)[39] than in the bulk causing rapid conversion of $NO_{2(ads)}$ (Figure S2D) back to $NO_3^-{}_{(ads)}$ (Figure S2C). Along with NO_2 emissions to the gas phase (Figure S2E),[65] heterogeneous NO_2 hydrolysis provides an extremely efficient sink for the consumption of $NO_{2(ads)}$.[38,39,66] As a result, the concentration of NO_2 in the surface layer (Figure S2D) remains much smaller (i.e., ~500-

fold smaller) than that in bulk ice (Figure S2B) as it is dictated by the quasi-stationary state between the adsorption/desorption, photolysis/hydrolysis and surface/bulk diffusion kinetics (Figure S3). Globally, the complex coupled kinetics at the air-ice interface result in the formation of a strong NO_2 concentration gradient through a thin photochemically active layer at the ice surface (i.e., $[NO_2] \propto \{1\text{-}\exp(-L/L^*)\}$ with $L^* \sim 5$ (8) nm for noon-time (night-time) conditions; see Figure S4). This gradient thus drives the NO_2 diffusive flux from bulk ice to the surface layer thereby feeding the photochemical NO_2 emissions that emanate from ice to the snowpack interstitial air.

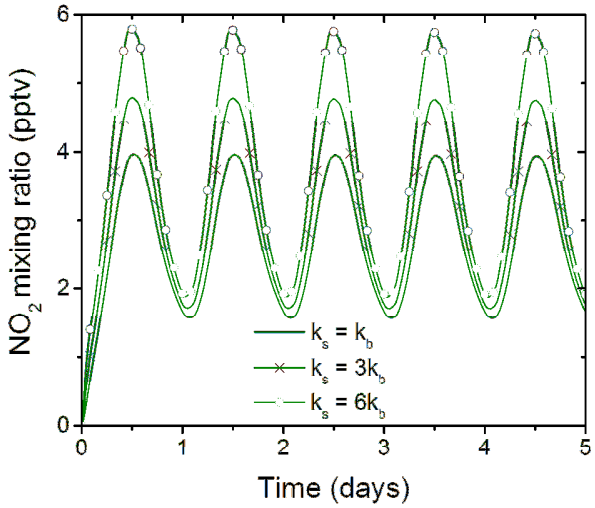

Fig. 4. Kinetic modelling results of the evolution in the interstitial air NO_2 mixing ratio resulting from the photochemical NO_2 emissions from ice. A 3(6)-fold enhancement in photolysis rates for surface nitrates (i.e., nitrates adsorbed onto the topmost layer at the interstitial air/ice interface, see Figure 3) increases the amplitude of the direct NO_2 photochemical emissions yielding a 30%(60%) increase in NO_2 mixing ratio ($k_s = 3k_b$; continuous line with x; $k_s = 6k_b$; continuous line with ○) compared to simulations where the bulk and surface rates are identical ($k_s = k_b$; continuous line without symbols). No attempt was made to reproduce the NO_2 mixing ratios nor the NO_2 photochemical fluxes measured in field campaign[7] to avoid introducing subjective biases in the model. However, since there exists large uncertainties in the NO_2 diffusion coefficients and hydrolysis rate constants required to model emissions, a sensitivity analysis was performed demonstrating the relative increase in photochemical emissions due to enhanced heterogeneous nitrates photolysis is robust with respect to a wide range in their kinetic parameters (see Figure S5 in the Supplementary Information).

In order to further parse out the surface and bulk contributions to the total photochemical NO_2 emissions, Figure 4 compares simulation results where the surface nitrates and bulk nitrates photolysis rates are identical ($k_s = k_b$; continuous trace without symbols) to simulation results where the surface nitrates photolysis rates are enhanced 3-fold ($k_s = 3k_b$; continuous trace with x) and 6-fold ($k_s = 6k_b$; continuous trace with ○)[67] compared to the bulk. As shown in Figure 4 (and described in details in the Supplementary information), a 3(6)-fold enhancement in nitrates photolysis rates at the surface of ice increases the amplitude of the diurnal cycles in NO_2 mixing ratios by 30%(60%)

comparatively to those where the bulk and surface photolysis rates are identical. Therefore, despite the relatively small 1:2999 surface-to-volume ratio used in the model, 25%(40%) of the photochemical NO_2 flux originate from surface-enhanced nitrates photolysis in the single, top-most layer at the ice surface. The fact that the photochemically active surface layer on ice is only L*~5-8 nm thick (Figure S4) therefore magnifies the contribution from enhanced photolysis of surface-bound nitrates to the NO_2 emissions to the snowpack interstitial air. We stress that this photochemically active layer *is not a QLL*, but rather consists of the ~3-5 superficial ice layers, including the top-most surface layer on ice where nitrate photolysis is enhanced by its heterogeneous solvation environment. These observations strongly suggest that bulk ice transport kinetics, in concert with enhanced surface nitrates photolysis/NO_2 hydrolysis, could have a major impact on the photochemical NO_x emissions to the polar boundary layer. Their explicit treatment in future modelling and simulation work might be required to qualitatively capture and adequately describe the surface and bulk contributions to heterogeneous ice (photo)chemistry in order to better understand the mechanism and rates responsible for the intense photochemical NO_x emissions from the snowpack to the polar boundary layer.

IV. Summary and Conclusions.

The link between the enhancement in photolysis rate for nitrates adsorbed onto a disordered ice surface and their intramolecular geometrical distortion provided a molecular-level understanding of this key heterogeneous atmospheric chemistry process. This phenomenon was shown to impact the complex coupled interfacial kinetics yielding a substantial increase in the photochemical NO_2 emissions from ice to the interstitial air. The surface-enhanced heterogeneous NO_2 hydrolysis and rapid NO_2 desorption from the surface layer (i.e., both processes acting as strong NO_2 sinks) cause the formation of a strongly depleted zone at the interstitial air/ice interface which is characterized by a steep NO_2 concentration gradient. This concentration gradient drives the diffusive NO_2 flux from bulk ice to the surface layer thereby feeding the photochemical NO_2 emissions that emanate from this thin photochemically active layer at the air-ice interface to the snowpack interstitial air. The small thickness of the photochemically active layer therefore magnifies the impact of surface-enhanced heterogeneous nitrates photolysis to the total photochemical NO_2 emissions. We stress that this photochemically active layer is not a QLL, but rather consists of the ~3-5 superficial ice layers, including the top-most surface layer on ice where nitrate symmetry is broken by its heterogeneous solvation environment which, along with a yet to be determined contribution from enhanced quantum yields, significantly increases the nitrates photolysis rate.

Therefore, despite the relatively small surface-to-volume ratio of fresh snow, such an (admittedly modest) enhancement in nitrates photolysis at the surface of ice could nonetheless provide a sizable contribution to snow (photo)chemistry given the small thickness of the photochemically active surface layer (which is dictated by the complex coupled kinetics at the air-ice interface). Clearly, as our understanding of the mechanisms and rates of the individual (but strongly coupled) elementary processes such as NO_2

diffusion and hydrolysis in bulk ice, as well as at its surface, will improve in the future, and measurements of heterogeneous nitrates photolysis under conditions more representative of the natural environment become available, we will be able to better describe the photochemical NO_x fluxes that emanate from the sunlit snowpack. Furthermore, other important but poorly understood heterogeneously catalyzed processes involved in the photochemical fluxes of reactive aldehydes and halogens species from the snowpack could also exhibit similar interfacial specificities. Eventually, explicit treatment of the complex coupled interfacial kinetics involved in heterogeneous (photo)chemistry on ice may thus help improve our description of polar boundary layer chemistry without resorting *de facto* to a QLL as the heterogeneous reaction medium.

V. Acknowledgments: We are grateful to NSERC (Canada) and CNRS (France) for financial support for this work. GM thanks FQRNT and EGIDE for doctoral fellowships. PA, PP and CL wish to acknowledge 65^e CPCFQ for support. PA thanks the Laboratoire de Chimie Physique – Matière et Rayonnement (Université Pierre et Marie Curie, Paris VI) for their hospitality during his sabbatical stay in Paris and Université de Sherbrooke for continued support. Very constructive comments and suggestions for reviewers are gratefully acknowledged.

Supporting Information Available: Detailed description of the kinetic model and selected results are provided as supplementary supporting information. This information is available free of charge via the Internet at http://pubs.acs.org.

Author Contributions: G.M., P.M., S.P., P.A., C.L., and P.P. designed and performed the experiments and analyzed the data. Kinetic modeling was performed by G.M. and P.A. The article was written by G.M., P.A., C.L., and P.P.

Competing financial interest: The authors declare no competing financial interest.

References and Notes:

(1) Honrath, R. E.; Peterson, M. C.; Guo, S.; Shepson, P. B.; Campbell, B. Evidence on NO_x Production within or upon Ice Particles in the Greenland Snowpack. *Geophys. Res. Lett.* **1999**, *26*, 695–698.

(2) Dominé, F.; Shepson, P. B. Air-Snow Interactions and Atmospheric Chemistry. *Science* **2002**, *297*, 1506–1510.

(3) Davis, D.; Chen, G.; Buhr, M.; Crawford, J.; Lenschow, D.; Lefer, B.; Shetter, R.; Eisele, F.; Mauldin, L.; Hogan, A. South Pole Chemistry: An Assessment of Factors Controlling Variability and Absolute Levels. *Atmos. Environ.* **2004**, *38*, 5375–5388.

(4) Eisele, F.; Davis, D.; Helmig, D.; Oltmans, S.; Neff, W.; Huey, G.; Tanner, D.; Chen, G.; Crawford, J.; Arimoto, R. Antarctic Tropospheric Chemistry Investigation (ANTCI) 2003 Overview. *Atmos. Environ.* **2008**, *42*, 2749–2761.

(5) Bauguitte, S. J.-B.; Bloss, W. J.; Evans, M. J.; Salmon, R. A.; Anderson, P. S.; Jones, A. E.; Lee, J. D.; Saiz-Lopez, A.; Roscoe, H. K.; Wolff, E. W.; et al. Summertime NO_x Measurements during the CHABLIS Campaign: Can Source and Sink Estimates Unravel Observed Diurnal Cycles? *Atmos. Chem. Phys.* **2012**, *12*, 989–1002.

(6) Honrath, R. E.; Peterson, M. C.; Dziobak, M. P.; Arsenault, M. A.; Green, S. A. Release of NO_x from Sunlight-Irradiated Midlatitude. *Geophys. Res. Lett.* **2000**, *27*, 2237–2240.

(7) Dibb, J. E.; Arsenault, M.; Peterson, M. C.; Honrath, R. E. Fast Nitrogen Oxide Photochemistry in Summit, Greenland Snow. *Atmos. Environ.* **2002**, *36*, 2501–2511.

(8) Berhanu, T. A.; Meusinger, C.; Erbland, J.; Jost, R.; Bhattacharya, S. K.; Johnson, M. S.; Savarino, J. Laboratory Study of Nitrate Photolysis in Antarctic Snow. II. Isotopic Effects and Wavelength Dependence. *J. Chem. Phys.* **2014**, *140*, 244306.

(9) Meusinger, C.; Berhanu, T. A.; Erbland, J.; Savarino, J.; Johnson, M. S. Laboratory Study of Nitrate Photolysis in Antarctic Snow. I. Observed Quantum Yield, Domain of Photolysis, and Secondary Chemistry. *J. Chem. Phys.* **2014**, *140*, 244305.

(10) Chu, L.; Anastasio, C. Quantum Yields of Hydroxyl Radical and Nitrogen Dioxide from the Photolysis of Nitrate on Ice. *J. Phys. Chem. A* **2003**, *107*, 9594–9602.

(11) Boxe, C. S.; Colussi, A. J.; Hoffmann, M. R.; Murphy, J. G.; Wooldridge, P. J.; Bertram, T. H.; Cohen, R. C. Photochemical Production and Release of Gaseous NO_2 from Nitrate-Doped Water Ice. *J. Phys. Chem. A* **2005**, *109*, 8520–8525.

(12) Dubowski, Y.; Colussi, A. J.; Hoffmann, M. R. Nitrogen Dioxide Release in the 302 nm Band Photolysis of Spray-Frozen Aqueous Nitrate Solutions. Atmospheric Implications. *J. Phys. Chem. A* **2001**, *105*, 4928–4932.

(13) Boxe, C. S.; Colussi, A. J.; Hoffmann, M. R.; Perez, I. M.; Murphy, J. G.; Cohen, R. C. Kinetics of NO and NO_2 Evolution from Illuminated Frozen Nitrate Solutions. *J. Phys. Chem. A* **2006**, *110*, 3578–3583.

(14) Jacobi, H.-W.; Annor, T.; Quansah, E. Investigation of the Photochemical Decomposition of Nitrate, Hydrogen Peroxide, and Formaldehyde in Artificial Snow. *J. Photochem. Photobiol. A Chem.* **2006**, *179*, 330–338.

(15) Zhu, C.; Xiang, B.; Chu, L. T.; Zhu, L. 308 nm Photolysis of Nitric Acid in the Gas Phase, on Aluminum Surfaces, and on Ice Films. *J. Phys. Chem. A* **2010**, *114*, 2561–2568.

(16) Frey, M. M.; Brough, N.; France, J. L.; Anderson, P. S.; Traulle, O.; King, M. D.; Jones, A. E.; Wolff, E. W.; Savarino, J. The Diurnal Variability of Atmospheric Nitrogen Oxides (NO and NO_2) above the Antarctic Plateau Driven by Atmospheric Stability and Snow Emissions. *Atmos. Chem. Phys.* **2013**, *13*, 3045–3062.

(17) Grannas, A. M.; Jones, A. E.; Dibb, J.; Ammann, M.; Anastasio, C.; Beine, H. J.; Bergin, M.; Bottenheim, J.; Boxe, C. S.; Carver, G.; et al. An Overview of Snow Photochemistry: Evidence, Mechanisms and Impacts. *Atmos. Chem. Phys. Discuss.* **2007**, *7*, 4165–4283.

(18) Thomas, J. L.; Stutz, J.; Lefer, B.; Huey, L. G.; Toyota, K.; Dibb, J. E.; von Glasow, R. Modeling Chemistry in and above Snow at Summit, Greenland – Part 1: Model Description and Results. *Atmos. Chem. Phys.* **2011**, *11*, 4899–4914.

(19) Boxe, C. S.; Saiz-Lopez, A. Multiphase Modeling of Nitrate Photochemistry in the Quasi-Liquid Layer (QLL): Implications for NO_x Release from the Arctic and Coastal Antarctic Snowpack. *Atmos. Chem. Phys. Discuss.* **2008**, *8*, 6009–6034.

(20) Jones, A. E.; Weller, R.; Wolff, E. W.; Jacobi, H.-W. Speciation and Rate of Photochemical NO and NO_2 Production in Antarctic Snow. *Geophys. Res. Lett.* **2000**, *27*, 345–348.

(21) Grannas, A. M.; Bausch, A. R.; Mahanna, K. M. Enhanced Aqueous Photochemical Reaction Rates after Freezing. *J. Phys. Chem. A* **2007**, *111*, 11043–11049.

(22) Thomas, J. L.; Dibb, J. E.; Huey, L. G.; Liao, J.; Tanner, D.; Lefer, B.; von Glasow, R.; Stutz, J. Modeling Chemistry in and above Snow at Summit, Greenland – Part 2: Impact of Snowpack Chemistry on the Oxidation Capacity of the Boundary Layer. *Atmos. Chem. Phys.* **2012**, *12*, 6537–6554.

(23) Sazaki, G.; Zepeda, S.; Nakatsubo, S.; Yokomine, M.; Furukawa, Y. Quasi-Liquid Layers on Ice Crystal Surfaces Are Made up of Two Different Phases. *Proc. Natl. Acad. Sci. U. S. A.* **2011**, *109*, 1052–1055.

(24) Sazaki, G.; Zepeda, S.; Nakatsubo, S.; Yokoyama, E.; Furukawa, Y. Elementary Steps at the Surface of Ice Crystals Visualized by Advanced Optical Microscopy. *Proc. Natl. Acad. Sci. U. S. A.* **2010**, *107*, 19702–19707.

(25) Bartels-Rausch, T.; Jacobi, H.-W.; Kahan, T. F.; Thomas, J. L.; Thomson, E. S.; Abbatt, J. P. D.; Ammann, M.; Blackford, J. R.; Bluhm, H.; Boxe, C.; et al. A Review of Air–ice Chemical and Physical Interactions (AICI): Liquids, Quasi-Liquids, and Solids in Snow. *Atmos. Chem. Phys.* **2014**, *14*, 1587–1633.

(26) Domine, F.; Bock, J.; Voisin, D.; Donaldson, D. J. Can We Model Snow Photochemistry? Problems with the Current Approaches. *J. Phys. Chem. A* **2013**, *117*, 4733–4749.

(27) Smith, R. S.; Kay, B. D. The Existence of Supercooled Liquid Water at 150 K. *Nature* **1999**, *398*, 788–791.

(28) Mishima, O.; Stanley, H. E. The Relationship between Liquid , Supercooled and Glassy Water. *Nature* **1998**, *396*, 329–335.

(29) Domine, F.; Albert, M.; Huthwelker, T.; Jacobi, H.-W.; Kokhanovsky, A. A.; Lehning, M.; Picard, G.; Simpson, W. R. Snow Physics as Relevant to Snow Photochemistry. *Atmos. Chem. Phys. Discuss.* **2008**, *8*, 171–208.

(30) Bartels-Rausch, T.; Donaldson, D. J. HONO and NO_2 Evolution from Irradiated Nitrate-Doped Ice and Frozen Nitrate Solutions. *Atmos. Chem. Phys. Discuss.* **2006**, *6*, 10713–10731.

(31) Baergen, A. M.; Donaldson, D. J. Photochemical Renoxification of Nitric Acid on Real Urban Grime. *Environ. Sci. Technol.* **2013**, *47*, 815–820.

(32) Wingen, L. M.; Moskun, A. C.; Johnson, S. N.; Thomas, J. L.; Roeselová, M.; Tobias, D. J.; Kleinman, M. T.; Finlayson-Pitts, B. J. Enhanced Surface Photochemistry in Chloride-Nitrate Ion Mixtures. *Phys. Chem. Chem. Phys.* **2008**, *10*, 5668–5677.

(33) Richards, N. K.; Wingen, L. M.; Callahan, K. M.; Nishino, N.; Kleinman, M. T.; Tobias, D. J.; Finlayson-Pitts, B. J. Nitrate Ion Photolysis in Thin Water Films in the Presence of Bromide Ions. *J. Phys. Chem. A* **2011**, *115*, 5810–5821.

(34) Schuttlefield, J.; Rubasinghege, G.; El-Maazawi, M.; Bone, J.; Grassian, V. H. Photochemistry of Adsorbed Nitrate. *J. Am. Chem. Soc.* **2008**, *130*, 12210–12211.

(35) Roca, M.; Zahardis, J.; Bone, J.; El-Maazawi, M.; Grassian, V. H. 310 nm Irradiation of Atmospherically Relevant Concentrated Aqueous Nitrate Solutions: Nitrite Production and Quantum Yields. *J. Phys. Chem. A* **2008**, *112*, 13275–13281.

(36) Nissenson, P.; Knox, C. J. H.; Finlayson-Pitts, B. J.; Phillips, L. F.; Dabdub, D. Enhanced Photolysis in Aerosols: Evidence for Important Surface Effects. *Phys. Chem. Chem. Phys.* **2006**, *8*, 4700–4710.

(37) Finlayson-Pitts, B. J. Reactions at Surfaces in the Atmosphere: Integration of Experiments and Theory as Necessary (but Not Necessarily Sufficient) for Prediction the Physical Chemistry of Aerosols. *Phys. Chem. Chem. Phys.* **2009**, *11*, 7760–7779.

(38) Svensson, R.; Ljungstrom, E.; Lindqvist, O. Kinetics of the Reaction between Nitrogen Dioxide and Water Vapour. *Atmos. Environ.* **1987**, *21*, 1529–1539.

(39) Finlayson-Pitts, B. J.; Wingen, L. M.; Sumner, A. L.; Syomin, D.; Ramazan, K. A. The Heterogeneous Hydrolysis of NO_2 in Laboratory Systems and in Outdoor and Indoor Atmospheres: An Integrated Mechanism. *Phys. Chem. Chem. Phys.* **2003**, *5*, 223–242.

(40) Cheung, J. L.; Li, Y. Q.; Boniface, J.; Shi, Q.; Davidovits, P.; Worsnop, D. R.; Jayne, J. T.; Kolb, C. E. Heterogeneous Interactions of NO_2 with Aqueous Surfaces. *J. Phys. Chem. A* **2000**, *104*, 2655–2662.

(41) Galbavy, E. S.; Anastasio, C.; Lefer, B. L.; Hall, S. R. Light Penetration in the Snowpack at Summit, Greenland: Part 1. *Atmos. Environ.* **2007**, *41*, 5077–5090.

(42) Dubowski, Y.; Colussi, A. J.; Boxe, C.; Hoffmann, M. R. Monotonic Increase of Nitrite Yields in the Photolysis of Nitrate in Ice and Water between 238 and 294 K. *J. Phys. Chem. A* **2002**, *106*, 6967–6971.

(43) Thogersen, J.; Réhault, J.; Odelius, M.; Ogden, T.; Jena, N. K.; Jensen, S. J. K.; Keiding, S. R.; Helbing, J. Hydration Dynamics of Aqueous Nitrate. *J. Phys. Chem. B* **2013**, *117*, 3376–3388.

(44) Relph, R. A.; Bopp, J. C.; Johnson, M. A.; Viggiano, A. A. Argon Cluster-Mediated Isolation and Vibrational Spectra of Peroxy and Nominally D_{3h} Isomers of CO_3^- and NO_3^-. *J. Chem. Phys.* **2008**, *129*, 064305.

(45) Goebbert, D. J.; Garand, E.; Wende, T.; Bergmann, R.; Meijer, G.; Asmis, K. R.; Neumark, D. M. Infrared Spectroscopy of the Microhydrated Nitrate Ions $NO_3^- \cdot (H_2O)_{(1-6)}$. *J. Phys. Chem. A* **2009**, *113*, 7584–7592.

(46) Hudson, P. K.; Schwarz, J.; Baltrusaitis, J.; Gibson, E. R.; Grassian, V. H. A Spectroscopic Study of Atmospherically Relevant Concentrated Aqueous Nitrate Solutions. *J. Phys. Chem. A* **2007**, *111*, 544–548.

(47) Waterland, M. R.; Stockwell, D.; Kelley, A. M. Symmetry Breaking Effects in NO_3^-: Raman Spectra of Nitrate Salts and Ab Initio Resonance Raman Spectra of Nitrate–water Complexes. *J. Chem. Phys.* **2001**, *114*, 6249.

(48) Kamboures, M. A.; Raff, J. D.; Miller, Y.; Phillips, L. F.; Finlayson-Pitts, B. J.; Gerber, R. B. Complexes of HNO_3 and NO_3^- with NO_2 and N_2O_4, and Their Potential Role in Atmospheric HONO Formation. *Phys. Chem. Chem. Phys.* **2008**, *10*, 6019–6032.

(49) Bianco, R.; Wang, S.; Hynes, J. T. Infrared Signatures of HNO_3 and NO_3^- at a Model Aqueous Surface. A Theoretical Study. *J. Phys. Chem. A* **2008**, *112*, 9467–9476.

(50) Ramesh, S. G.; Re, S.; Boisson, J.; Hynes, J. T. Vibrational Symmetry Breaking of NO_3^- in Aqueous Solution: NO Asymmetric Stretch Frequency Distribution and Mean Splitting. *J. Phys. Chem. A* **2010**, *114*, 1255–1269.

(51) Thibert, E.; Domine, F. Thermodynamics and Kinetics of the Solid Solution of HNO_3 in Ice. *J. Phys. Chem. B* **1998**, *102*, 4432–4439.

(52) Marcotte, G.; Ayotte, P.; Bendounan, A.; Sirotti, F.; Laffon, C.; Parent, P. Dissociative Adsorption of Nitric Acid at the Surface of Amorphous Solid Water Revealed by X-Ray Absorption Spectroscopy. *J. Phys. Chem. Lett.* **2013**, *4*, 2643–2648.

(53) Ellis, S. R. M.; Thwaites, J. M. Vapour-Liquid Equilibria of Nitric Acid-Water-Sulfuric Acid Mixtures. *J. Appl. Chem.* **1957**, *7*, 152–160.

(54) Stevenson, K. P.; Kimmel, G. A.; Dohnàlek, Z.; Smith, R. S.; Kay, B. D. Controlling the Morphology of Amorphous Solid Water. *Science* **1999**, *283*, 1505–1507.

(55) Marchand, P.; Marcotte, G.; Ayotte, P. Spectroscopic Study of HNO_3 Dissociation on Ice. *J. Phys. Chem. A* **2012**, *116*, 12112–12122.

(56) Pronovost, S. Études Des Phénomènes Photochimiques Des Nitrates et Analyse de La Cinétique Lors de La Photolyse de L'acide Nitrique, Master's Thesis, Univesité de Sherbrooke, 2012, p. 116.

(57) Mack, J.; Bolton, J. R. Photochemistry of Nitrite and Nitrate in Aqueous Solution : A Review. *J. Photochem. Photobiol. A Chem.* **1999**, *128*, 1–13.

(58) King, M. D.; Simpson, W. R. Extinction of UV Radiation in Arctic Snow at Alert, Canada (82°N). *J. Geophys. Res.* **2001**, *106*, 12,499–12,507.

(59) While photolysis quantum yields could be estimated from these experimentally determined effective photolysis rates, this would require making assumptions about the UV absorption cross sections of surface and bulk nitrates as well as about the spectral irradiance within the film and at its surface. We therefore chose to compare effective photolysis rates for surface nitrates and bulk nitrates under otherwise identical experimental conditions (aside from the sample preparation procedure). Experiments are currently underway that aim at providing the absorption cross sections required in order to quantify surface nitrates and bulk nitrates photolysis quantum yields.

(60) Bianco, R.; Wang, S.; Hynes, J. T. Theoretical Study of the Dissociation of Nitric Acid at a Model Aqueous Surface. *J. Phys. Chem. A* **2007**, *111*, 11033–11042.

(61) Svoboda, O.; Kubelová, L.; Slavíček, P. Enabling Forbidden Processes: Quantum and Solvation Enhancement of Nitrate Anion UV Absorption. *J. Phys. Chem. A* **2013**, *117*, 12868–12877.

(62) Svoboda, O.; Slavíček, P. Is Nitrate Anion Photodissociation Mediated by Singlet-Triplet Absorption ? *J. Phys. Chem. Lett.* **2014**.

(63) Gvozdić, V.; Tomišić, V.; Butorac, V.; Simeon, V. Association of Nitrate Ion with Metal Cations in Aqueous Solution : A UV-Vis Spectrometric and Factor-Analytical Study. *Croat. Chem. Acta* **2009**, *82*, 553–559.

(64) Honrath, R. E.; Lu, Y.; Peterson, M. C.; Dibb, J. E.; Arsenault, M. A.; Cullen, N. J.; Steffen, K. Vertical Fluxes of NO_x, HONO, and HNO_3 above the Snowpack at Summit , Greenland. *Atmos. Environ.* **2002**, *36*, 2629–2640.

(65) Bartels-Rausch, T.; Eichler, B.; Zimmermann, P.; Ammann, M. The Adsorption Enthalpy of Nitrogen Oxides on Crystalline Ice. *Atmos. Chem. Phys.* **2002**, *2*, 235–247.

(66) Krepelová, A.; Newberg, J.; Huthwelker, T.; Bluhm, H.; Ammann, M. The Nature of Nitrate at the Ice Surface Studied by XPS and NEXAFS. *Phys. Chem. Chem. Phys.* **2010**, *12*, 8870–8880.

(67) An enhancement of this magnitude is displayed by the most distorted nitrates at the surface of ice (i.e., those that display a 200-250 cm^{-1} gap in their asym-$NO_{str.}$ splitting.